physica status solidi a
www.pss-a.com

Binary Addressable Optical Multiplexing Waveguides via Electrochromic Switching

*Seon-Young Rhim, Max Heyl, Kurt Busch, and Emil J.W. List-Kratochvil**

Photonic circuits attract much attention as promising candidates to overcome the drawbacks of their electronic counterparts. By utilizing the broad bandwidth and low energy consumption of optical communication, hybrid circuits can provide a comprehensive platform for the era beyond Moore's law. In particular, parallel matrix operations, the heavy lifting behind neural networks, remain challenging for traditional electronics due to high heat dissipation. To enable these parallel computations optically, (de-)multiplexing is crucial to address the different channels. Previously this has been accomplished with complex spectral or time encodings in wave division or time division methods. However, herein, a simple method to address parallel optical channels exclusively with 2-bit signals is presented. By using PEDOT:PSS as electrochromic material for intensity modulation, light transmission or absorption is controlled by oxidation and reduction with an electrolyte. Y-branch structures are used to design the multiplexing layout and to assign the 2-bit states to the channels. This binary addressable optical multiplexer, therefore, combines optical communication with electronic signals into a hybrid circuit.

1. Introduction

In the last decade, optical communication paved its way more and more toward information technology. While in the 20th century, electronic signals were mainly used as the information carrier, optical fibers made with transparent dielectric materials are nowadays replacing metallic cables as the information-carrying medium. Moreover, with their broad bandwidth and low power consumption, photonic integrated chips enabled by structured light propagating waveguides, became a competitive counterpart to traditional electronics.[1] In general, such photonic systems exploit light modulation through phase, intensity, and polarization to en- and decode information for signal processing.[2] With specific topological waveguide structures, mathematical operations such as differential functions, Fourier transforms, and multiply-accumulate computations could be realized in an analog fashion, for which electronics require a large computational capacity.[3] Especially, optical neuromorphic engineering is a promising candidate to surpass the von Neumann-based neural network simulations due to their advantages of large parallel operations and low power consumption.[4] In such optical devices, addressing different channels is one of the key parts affecting performance. Therefore, various optical neuromorphic devices were reported by using different optical multiplexing methods.[5] The most common methods of addressing single channels optically are wavelength division multiplexing (WDM) and time division multiplexing (TDM).[6] While WDM assigns single channels with different wavelengths by interference, TDM uses pulse timing by designing different optical path lengths for each waveguide channel. However, both are subject to high requirements regarding fabrication and output detection, since a spectral or time encoding is needed respectively.

Therefore, in this work, we demonstrate a simple method for optical multiplexing via intensity modulation to address each single channel exclusively by using digital signals as schematically shown in **Figure 1**a. By connecting two Y-branch layers in series (layers 1 and 2), 2-bit (one-to-four) demultiplexing was demonstrated. For this purpose, we utilized the coloring and bleaching effect of electrochromic (EC) materials to control the intensity of the propagating light in waveguides. Distinct to the phase modulation, electrochromic materials like PEDOT:PSS and tungsten oxide (WO_3) exhibit a broad absorption peak in the visible and in

S.-Y. Rhim, M. Heyl, E. J. W. List-Kratochvil
Institut für Physik
Institut für Chemie & IRIS Adlershof
Humboldt-Universität zu Berlin
Zum Großen Windkanal 2, 12489 Berlin, Germany
E-mail: emil.list-kratochvil@hu-berlin.de

K. Busch
Institut für Physik
Humboldt-Universität zu Berlin
Zum Großen Windkanal 2, 12489 Berlin, Germany

K. Busch
Max-Born-Institut für Nichtlineare Optik und Kurzzeitspektroskopie
Max-Born-Straße 2A, 12489 Berlin, Germany

E. J. W. List-Kratochvil
Helmholtz-Zentrum für Materialien und Energie GmbH
Hahn-Meitner-Platz 1, 14109 Berlin, Germany

The ORCID identification number(s) for the author(s) of this article can be found under https://doi.org/10.1002/pssa.202300177.

DOI: 10.1002/pssa.202300177

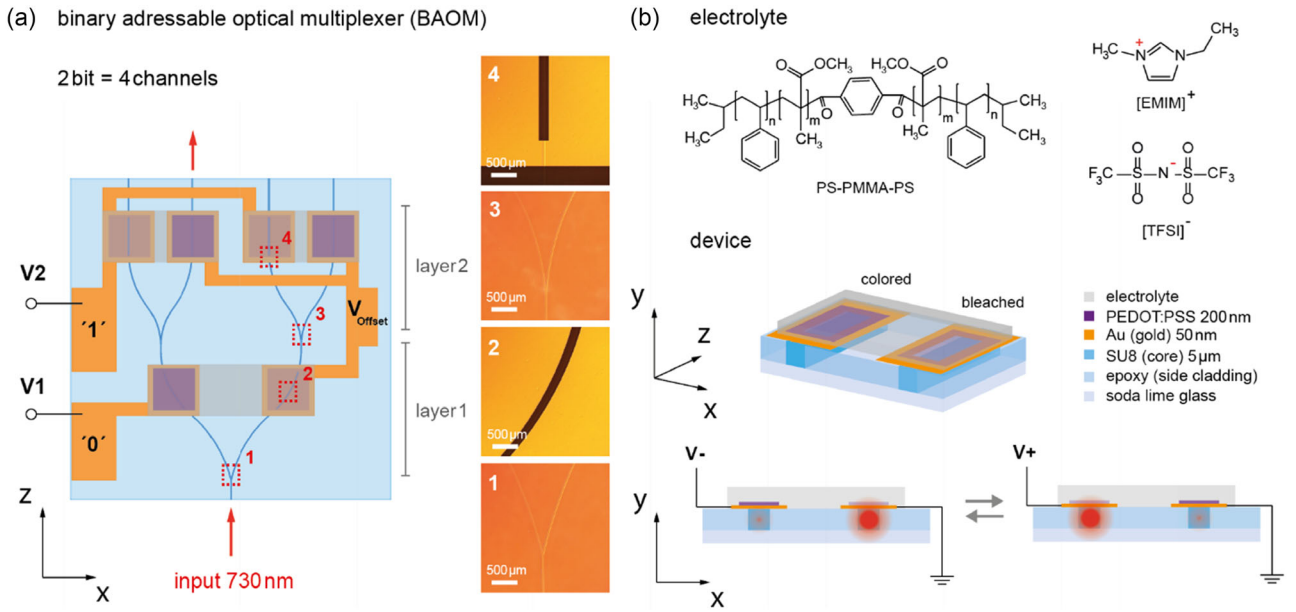

Figure 1. a) Schematic picture of the binary addressable optical (de-)multiplexer (BAOM) consisting of two layers of y-branches connected in series. Channels can be addressed by applying voltages on V1 (first bit) and V2 (second bit) according to the 2-bit state. The microscope pictures show the branches and the electrodes of the device. The V_{offset} is the logic supply, with which the voltage level of the 2-bit code is controlled. b) Cross-sectional view of the paired waveguides. At the top, the chemical structure of the utilized ion gel electrolyte is presented. The picture at the bottom shows light transmission of either the right or left waveguide depending on the coloring and bleaching of the electrochromic PEDOT:PSS according to the applied voltage.

the near-infrared region when reduced and are almost transparent when oxidized.[7] While already established in smart displays and windows, electrolyte-controlled EC effects on waveguides recently received more attention for novel applications in photonics.[8] By coating optical waveguides with EC materials, the intensity modulation is mediated by the evanescent field which appears at the waveguide borders and interacts with the surrounding materials. Furthermore, previous reports showed that the intensity modulation of the guided light is additionally enhanced by surface plasmon polariton (SPP) excitations. In brief, SPPs are electron oscillations coupled to electromagnetic fields, which propagate along a conductor–dielectric interface. Thus, since reduction (coloring) and oxidation (bleaching) by ion migration leads to a conductivity change of the EC material, SPP excitations are switched on and off increasing the modulation effect on the guided light.[8,9] In the presented device described in Figure 1, we used PEDOT:PSS as the EC material deposited on a 40 µm wide and 5 µm high-embedded SU-8 waveguide. As shown in Figure 1b, both arms of the same Y-branch were paired up together by an ion gel electrolyte, which allowed to address each arm exclusively with just one working electrode. A well-known mixture of the polymer poly(styrene-*block*-methylmethacrylate-*block*-styrene) (PS-PMMA-PS) and the ionic liquid (IL) 1-Ethyl-3-methylimidazolium bis(trifluoromethylsulfonyl)imide ([EMIM][TFSI]) was used to shift the ions between the optical arms.[10] To control the electric field, 50 nm thin gold electrodes were structured on the waveguide with an open window to enable a direct interaction between the guided light and the EC material PEDOT:PSS. For the measurement of the (de-)multiplexing device, lensed fibers were used at the in- and output together with a 730 nm light-emitting diode (LED) source and a charge-coupled device (CCD) detector.

2. Results and Discussion

2.1. Modulation Characteristics

To exploit the intensity modulation in waveguides for (de-) multiplexing, a single embedded SU-8 waveguide was first prepared to characterize the modulation behavior. For this purpose, PEDOT:PSS was deposited on a frame-like shaped gold electrode, which was directly structured on the waveguide. To control the coloring and the bleaching of the PEDOT:PSS, an additional counter electrode (ground) was used to shift the ions in and out of the EC material. As illustrated in **Figure 2**a, a positive bias triggers the TFSI anions to penetrate the EC material, resulting in bleaching in the visible and coloring in the infrared region through p-doping via oxidation of the PEDOT. The resulting radical cations and dications, or polarons and bipolarons, respectively, act as charge carriers filling up the energy gap with additional states in PEDOT, as shown in Figure S1, Supporting Information.[11] Whereas, a negative bias conducts a dedoping due to the reduction of the PEDOT, since the EMIM cations compensate the sulfonate groups.[12] Exploiting these effects, the light intensity of the waveguide can be modulated through the evanescent field E^2, as schematically shown in Figure 2a. In the colored state, the field intensity of the guided light drops exponentially with the overlap length between the EC material and the waveguide according to the Lambert–Beer law with an estimated

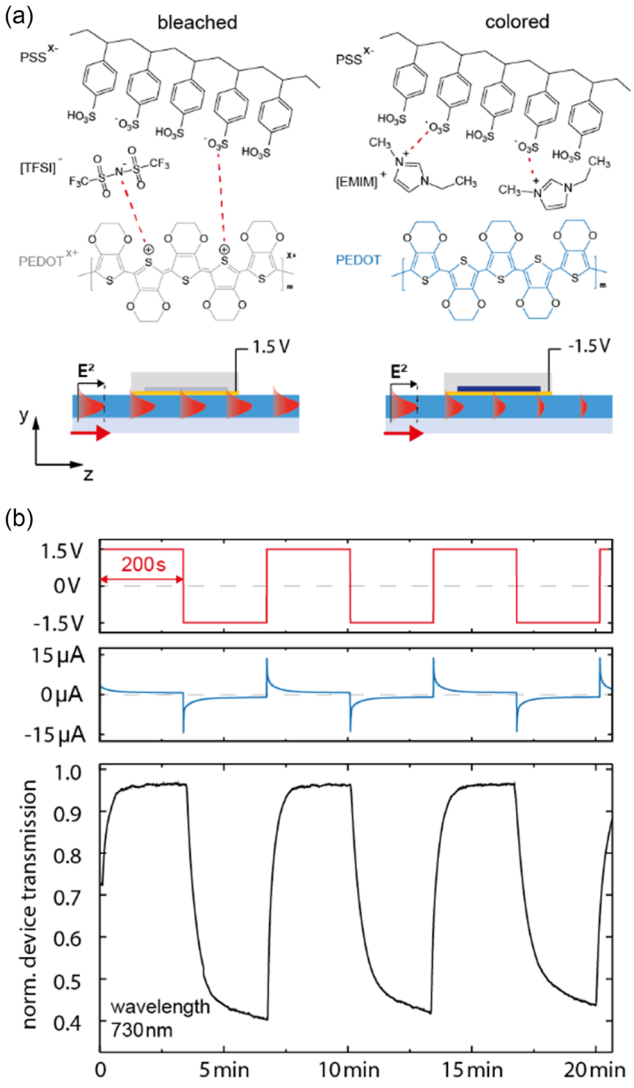

Figure 2. a) The chemical structure of the PEDOT:PSS when bleached (oxidized) by TFSI and colored (reduced) by EMIM cations. A cross-sectional view along the propagation direction of the waveguide illustrates the intensity progress of the propagating light in the bleached and colored state. b) Transmission modulation diagram at 730 nm wavelength upon the applied voltage sequence and the corresponding current.

extinction coefficient of 0.32 mm^{-1} at 730 nm wavelength.[13] As shown in Figure 2b, by alternating the voltage every 200 s between 1.5 and −1.5 V against the grounded counter electrode, an ionic current of about 15 µA at the peak was observed when the electric field direction was reversed. Thereby, the normalized transmission at 730 nm exhibited a modulation range of about 55% on a single device. The operation wavelength was chosen based on absorption spectrum of bleached and colored state in Figure S3, Supporting Information revealing the highest modulation at 730 nm wavelength in the visible region. As evident by the ionic current decay, the transmission was mainly modulated in the first 30 s of the field reversal thus showing a rectangular shape in the transmission-time diagram. Furthermore, Figure S4, Supporting Information exhibits device performance of 1,000 switches utilizing a sandwiched-sealed aqueous lithium triflate electrolyte on the same waveguide structure, demonstrating the high reliability of PEDOT:PSS in terms of transmission modulation. This observation corresponds with various prior studies.[14]

2.2. Proof of Concept: Binary Addressable Optical (De-) multiplexer (BAOM)

Applying the elaborated results of the single device (Figure 2) toward a (de-)multiplexer device, as shown in Figure 1a, a BAOM can be designed. As mentioned in the introduction, pairing up the electrodes of both Y-branch arms by an electrolyte enables one to address each arm exclusively with just one working electrode. As soon as a field direction is applied, one arm opens up for light transmission while the other closes by absorption. Therefore, by connecting such Y-branches in series and connecting the electrodes of the same arms together (e.g., right arms), binary addressing is possible by assigning one bit to each Y-branch layer, as illustrated in Figure 1a.

Figure 3a shows a photo of the fabricated BAOM with two layers of Y-branches connected in series with two contact pads for each layer and a single contact for the offset voltage as the logic supply. To keep some carry-over to traditional electronics and thus to offer an interface between the electronics and optics, the voltage offset was set to 1.5 V to run the BAOM device with 3 and 0 V for the binary value 1 and 0, respectively. In this 2-bit driven device ($2^2 = 4$ states), the four channels can be thus addressed exclusively.

Figure 3b shows the utilized voltage sequences for V1 and V2 and the related current flow. The 2-bit state signals are marked as I, II, III, and IV, and each state was applied for 30 s. The schematic pictures on the left-hand side in Figure 3c identify the open channel regarding the applied 2-bit state. As chosen, the Roman numbers of the state coincide with the channel number (e.g., II = ch. 2).

On the right-hand side, the normalized transmission for each output channel is shown when BAOM was used as a demultiplexer. Channel 1 opened up when a voltage of 3 V was applied on both contacts, V1 and V2 (state I), and closed when a different 2-bit state (II, III, or IV) was used. The emphasized solid black line in the diagram exhibits the time progress of the measured transmission in channel 1 regarding the applied voltage sequence in Figure 2b. The normalized transmission reached 100% when the channel opened and fell down at least under 40% when closed. The transmission progress of channel 2 (red), channel 3 (dark-blue), and channel 4 (green) are also shown in Figure 3c and exhibits a similar behavior upon the same applied voltage sequence. Thus, for all four channels, sufficient light transmission was only observed when the channel was exclusively addressed. It is also worth mentioning that the presented device is appropriate to operate in near-infrared region commonly used in photonic communication. However, contrary to the results in the visible region, bleaching and coloring in the infrared region are reversed due to the polaron and bipolaron formation as mentioned in the prior section. Moreover, the proven functionality of the presented demultiplexer initially includes the function of a multiplexer when exchanging the input with the output (four-to-one).

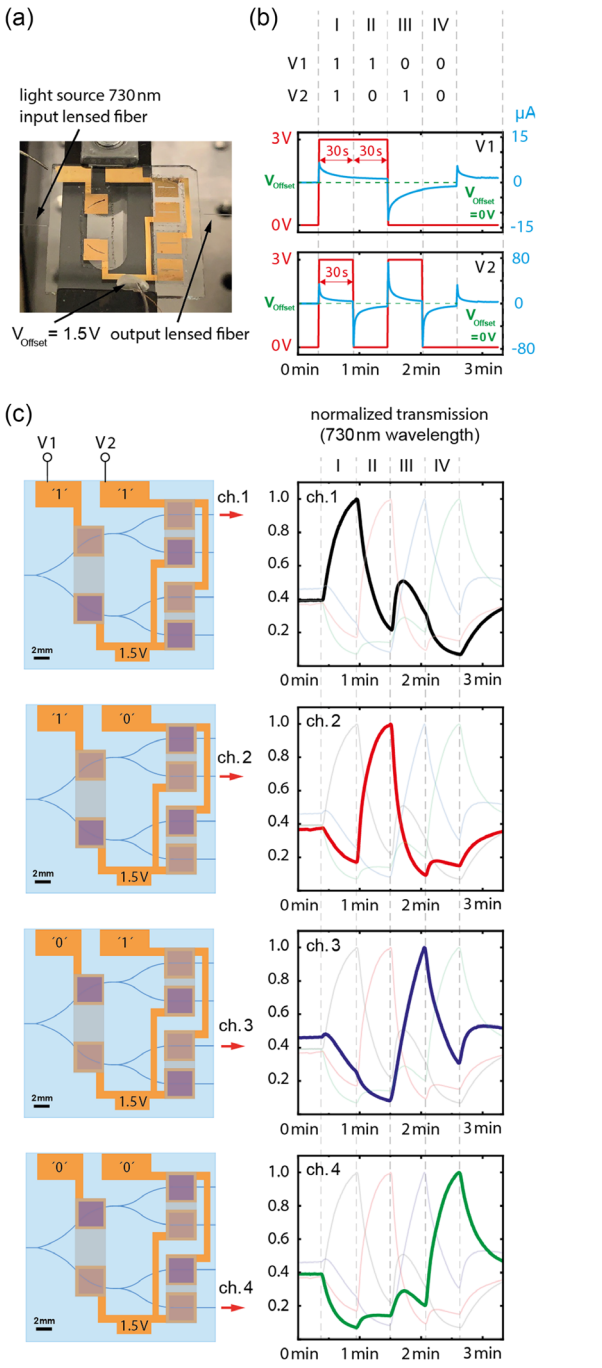

Figure 3. a) Photo of the fabricated BAOM device. b) Applied voltage sequence for V1 and V2 with the corresponding 2-bit states (I, II, III, and IV). c) (Left) Schematic pictures of the BAOM at different states, showing different constellations of the bleached (gray) and colored (purple) PEDOT:PSS with the corresponding opened channels. (Right) Transmission progress of channel 1 (black), channel 2 (red), channel 3 (blue), and channel 4 (green) upon the applied voltage sequence.

Particularly, in optical neuromorphics, controlling the intensity of several optical channels by fewer digital bits can reduce the complexity during synaptic weights adjustments. A higher modulation speed of the presented device can be generally achieved by using shorter but higher voltage pulses or an electrolyte with higher ionic conductivity. However, a higher voltage comes with the risk of electrochemical water splitting in the electrolyte and degradation of the PEDOT:PSS.[7d,15]

To date, various organic electrochemical transistors with PEDOT:PSS as the semiconductor material were reported in which the devices were switched on the milli- to microsecond scale by using aqueous solutions.[16] Although it is well-known that aqueous solutions with small ions like sodium (Na^+) or lithium (Li^+) cations exhibit a high ion mobility,[17] aqueous electrolytes are hard to handle due to the low viscosity and ambient factors like evaporation. In contrast, the chosen ion gel electrolyte in this work enables to operate in the atmosphere over a longer time period. Nevertheless, using smaller sodium or lithium-based salt molecules can also increase the ion mobility in ion gel electrolytes.[18] Also, geometrical factors like device miniaturization can improve the speed performance of the device by shortening the distance between the electrodes. Furthermore, by modifying the waveguide shape down to single-mode sizes, the modulation range can be drastically enhanced. A higher total internal reflection density, which confines and guides light through dielectric materials, increases the extinction coefficient, facilitating a significantly smaller interaction area between the waveguide and the EC material. Considering these parameters, the proposed BAOM device can become a serious candidate for optical exclusive (de-)multiplexing.

3. Conclusion

In this work, a novel kind of device for simple optical (de-) multiplexing was demonstrated by combining the electrochromic material PEDOT:PSS with waveguides. The utilized layout consisted of two layers of Y-branches which were connected in series enabling a split into four channels. Two electrodes deposited with PEDOT:PSS on each arm of a Y-branch were paired up together by an ion gel electrolyte. By controlling just one of the paired electrodes, it was possible to address each channel exclusively through coloring and bleaching. The evanescent field thereby interacted with the electrochromic material PEDOT:PSS causing an in- and decrease of the light transmission in waveguides accordingly. Applying this effect on the proposed layout, a new method of optical multiplexing was demonstrated in which each channel can be exclusively addressed with a binary 2-bit signal.

4. Experimental Section

Fabrication of the Planar-Embedded Dielectric Waveguide: To fabricate a planar-embedded waveguide, a strip-off method was used. First, P3HT (Sigma-Aldrich, regioregular, $M_w = 20–45$ kg mol^{-1}) was dissolved in chlorobenzene with a concentration of 20 mg mL^{-1} and spin coated on a silicon substrate as the sacrificial layer. After activating the P3HT surface via O_2 plasma for few seconds, SU-8 TF6005 resist (Kayaku Advanced Materials Inc.) was spin coated on the P3HT layer to achieve a 5 μm thick and 40 μm wide waveguide structure via photolithography. Afterward, UV-curable epoxy (Ossila Inc.) was poured on the silicon substrate with the waveguide structure and then sandwiched with ozone-treated soda-lime glass substrate. After curing the epoxy through the glass substrate with UV (<400 nm) light for 2 hours, the sample was immersed in

chloroform to dissolve the P3HT sacrificial layer. Subsequently, the soda-lime glass with the planar embedded waveguide was detached off the silicon substrate and treated with O_2 plasma to remove P3HT residues.

Electrodes Structuring: The electrodes were structured via lift-off processing. For this purpose, the negative resist AZ nL of 2035 (MicroChemicals GmbH) was spin coated on the planar embedded waveguide and structured via photolithography. Afterward, 50 nm thick gold was evaporated on the structured sample. Subsequently, the gold was lifted-off by putting the sample in the remover (Technistrip NI555, MicroChemicals GmbH) for 12 h.

Preparation of the Ion Gel Electrolyte: Adapted from previous work,[10] the ion gel was prepared by combining the ionic liquid (IL) 1-ethyl-3 methylimidazolium bis(trifluoromethylsulfonyl)imide ([EMIM][TFSI], from IOLITEC) with the triblock copolymer poly(styrene-*block*-methylmethacrylate-*block*-styrene) (PS-PMMA-PS, from Polymer Source. Inc., Product ID: P18602-SMMAS, $M_w = 21.1\ \mathrm{kg\ mol^{-1}}$) using ethyl propionate (Sigma-Aldrich, 99%) as solvent. A 33 mg $\mathrm{mL^{-1}}$ polymer solution in ethyl propionate was prepared and the IL was added with an IL to polymer weight ratio of 75 wt%. To prepare the ion gel film, the solution was drop casted on the sample, followed by a drying step in a vacuum oven at 70 °C overnight. Subsequently, the electrolyte film was structured with a water-soaked cotton swab to pair up the electrodes together.

Supporting Information

Supporting Information is available from the Wiley Online Library or from the author.

Acknowledgements

The authors gratefully acknowledge financial support by the Deutsche Forschungsgemeinschaft through project no. 182087777—SFB 951. This work was carried out in the framework of the Joint Lab GEN_FAB and was supported by the HySPRINT Innovation Lab at Helmholtz-Zentrum Berlin.

Open Access funding enabled and organized by Projekt DEAL.

Conflict of Interest

The authors declare no conflict of interest.

Data Availability Statement

The data that support the findings of this study are available from the corresponding author upon reasonable request.

Keywords

electrochromic, electrolyte, multiplexing, photonics, waveguide

Received: March 13, 2023
Revised: June 26, 2023
Published online: August 2, 2023

[1] a) J. Wang, Y. Long, *Sci. Bull.* **2018**, *63*, 1267; b) D. Marpaung, J. Yao, J. Capmany, *Nat. Photonics* **2019**, *13*, 80; c) S. Y. Siew, B. Li, F. Gao, H. Y. Zheng, W. Zhang, P. Guo, S. W. Xie, A. Song, B. Dong, L. W. Luo, C. Li, X. Luo, G. Q. Lo, *J. Lightwave Technol.* **2021**, *39*, 4374.

[2] a) L. Jiang, J. Wu, Q. Li, G. Deng, X. Zhang, Z. Li, K. Chen, K. S. Chiang, *J. Mater. Chem. C* **2019**, *7*, 6257; b) S. Zhang, Z. Li, F. Xing, *Int. J. Mol. Sci.* **2020**, *21*, 1608; c) Z. Gong, F. Yang, L. Wang, R. Chen, J. Wu, C. P. Grigoropoulos, J. Yao, *J. Appl. Phys.* **2021**, *129*, 030902; d) I. Taghavi, M. Moridsadat, A. Tofini, S. Raza, N. A. F. Jaeger, L. Chrostowski, B. J. Shastri, S. Shekhar, *Nanophotonics* **2022**, *11*, 3855.

[3] a) Z. Cheng, R. Cao, J. Guo, Y. Yao, K. Wei, S. Gao, Y. Wang, J. Dong, H. Zhang, *Nanophotonics* **2020**, *9*, 1973; b) H. Zhou, Y. Zhao, X. Wang, D. Gao, J. Dong, X. Zhang, *ACS Photonics* **2020**, *7*, 792; c) M. A. Nahmias, T. F. De Lima, A. N. Tait, H. T. Peng, B. J. Shastri, P. R. Prucnal, *IEEE J. Sel. Top. Quantum Electron.* **2020**, *26*, 1; d) X. Guo, J. Xiang, Y. Zhang, Y. Su, *Adv. Photonics Res.* **2021**, *2*, 2000212.

[4] a) H. Zhang, J. Thompson, M. Gu, X. D. Jiang, H. Cai, P. Y. Liu, Y. Shi, Y. Zhang, M. F. Karim, G. Q. Lo, X. Luo, B. Dong, L. C. Kwek, A. Q. Liu, *ACS Photonics* **2021**, *8*, 1662; b) K. Berggren, Q. Xia, K. K. Likharev, D. B. Strukov, H. Jiang, T. Mikolajick, D. Querlioz, M. Salinga, J. R. Erickson, S. Pi, F. Xiong, P. Lin, C. Li, Y. Chen, *Nanotechnology* **2021**, *32*, 012002; c) B. Xu, Y. Huang, Y. Fang, Z. Wang, S. Yu, R. Xu, *Photonics* **2022**, *9*, 698; d) F. Ashtiani, A. J. Geers, F. Aflatouni, *Nature* **2022**, *606*, 501; e) S. Y. Rhim, G. Ligorio, F. Hermerschmidt, M. Pätzel, M. Herder, S. Hecht, E. J. W. List-Kratochvil, *J. Phys. D Appl. Phys.* **2022**, *55*, 044002.

[5] a) T. Ferreira De Lima, A. N. Tait, A. Mehrabian, M. A. Nahmias, C. Huang, H. T. Peng, B. A. Marquez, M. Miscuglio, T. El-Ghazawi, V. J. Sorger, B. J. Shastri, P. R. Prucnal, *Nanophotonics* **2020**, *9*, 4055; b) C. Wu, H. Yu, S. Lee, R. Peng, I. Takeuchi, M. Li, *Nat. Commun.* **2021**, *12*, 96; c) T. Fu, Y. Zang, Y. Huang, Z. Du, H. Huang, C. Hu, M. Chen, S. Yang, H. Chen, *Nat. Commun.* **2023**, *14*, 70.

[6] a) G. E. Keiser, *Opt. Fiber Technol.* **1999**, *5*, 3; b) A. A. Aboketaf, A. W. Elshaari, S. F. Preble, *Opt. InfoBase Conf. Papers* **2010**, *18*, 13529; c) Y. Huang, M. Badar, A. Nitkowski, A. Weinroth, N. Tansu, C. Zhou, *Biomed. Opt. Express* **2017**, *8*, 3856; d) L. Feng, M. Zhang, J. Wang, X. Zhou, X. Qiang, G. Guo, X. Ren, *Photonics Res.* **2022**, *10*, A135.

[7] a) D. Levasseur, I. Mjejri, T. Rolland, A. Rougier, *Polymers* **2019**, *11*, 179; b) J. T. Kim, J. Song, C. S. Ah, *ACS Appl. Electron. Mater.* **2020**, *2*, 2057; c) E. Hopmann, B. N. Carnio, C. J. Firby, B. Y. Shahriar, A. Y. Elezzabi, *Nano Lett.* **2021**, *21*, 1955; d) W. Wu, H. Zeng, W. Zhang, W. Zhang, H. Jiang, G. Wu, Z. Li, X. Wang, Y. Huang, Z. Lei, *J. Appl. Polym. Sci.* **2023**, *140*, e53211.

[8] E. Hopmann, B. Y. Shahriar, A. Y. Elezzabi, *Nanoscale* **2022**, *14*, 6526.

[9] a) A. Agrawal, C. Susut, G. Stafford, B. McMorran, H. Lezec, A. Alec Talin, *Opt. InfoBase Conf. Papers* **2011**, *11*, 2774; b) J. T. Kim, J. Song, H. Ryu, C. S. Ah, *Adv. Opt. Mater.* **2020**, *8*, 1901464.

[10] a) J. Pu, Y. Yomogida, K.-k. Liu, L.-j. Li, Y. Iwasa, T. Takenobu, *Nano Lett.* **2012**, *12*, 4013; b) Y. Yomogida, J. Pu, H. Shimotani, S. Ono, S. Hotta, Y. Iwasa, T. Takenobu, *Adv. Mater.* **2012**, *24*, 4392.

[11] a) N. Massonnet, A. Carella, O. Jaudouin, P. Rannou, G. Laval, C. Celle, J. P. Simonato, *J.Mater. Chem. C* **2014**, *2*, 1278; b) R. Brooke, E. Mitraka, S. Sardar, M. Sandberg, A. Sawatdee, M. Berggren, X. Crispin, M. P. Jonsson, *J. Mater. Chem. C* **2017**, *5*, 5824.

[12] a) M. Marzocchi, I. Gualandi, M. Calienni, I. Zironi, E. Scavetta, G. Castellani, B. Fraboni, *ACS Appl. Mater. Interfaces* **2015**, *7*, 17993; b) S. Fabiano, N. Sani, J. Kawahara, L. Kergoat, J. Nissa, I. Engquist, X. Crispin, M. Berggren, *Sci. Adv.* **2017**, *3*, 1700345.

[13] a) M. Vlk, A. Datta, S. Alberti, H. D. Yallew, V. Mittal, G. S. Murugan, J. Jágerská, *Light Sci. Appl.* **2021**, *10*, 26; b) P. Neutens, R. Jansen, G. Woronoff, M. Rutowska, N. Hosseini, F. Buja, A. Humbert, F. Colle, T. Stakenborg, W. Van Roy, *Biomed. Opt. Express* **2021**, *12*, 2041.
[14] a) T. A. Welsh, E. R. Draper, *RSC Adv.* **2021**, *11*, 5245; b) H. Jiang, W. Wu, Z. Chang, H. Zeng, R. Liang, W. Zhang, W. Zhang, G. Wu, Z. Li, H. Wang, *E-Polymers* **2021**, *21*, 722.
[15] a) P. Bogdanoff, D. Stellmach, O. Gabriel, B. Stannowski, R. Schlatmann, R. van de Krol, S. Fiechter, *Energy Technol.* **2016**, *4*, 230; b) J. Fan, S. S. Rezaie, M. Facchini-Rakovich, D. Gudi, C. Montemagno, M. Gupta, *Org. Electron.* **2019**, *66*, 148; c) D. J. Yun, J. Jung, Y. M. Sung, H. Ra, J. M. Kim, J. G. Chung, S. Y. Kim, Y. S. Kim, S. Heo, K. H. Kim, Y. J. Jeong, J. Jang, *Adv. Electron. Mater.* **2020**, *6*, 2000620; d) J. Pan, M. Liu, D. Li, H. Zheng, D. Zhang, *J. Pharm. Anal.* **2021**, *11*, 699.
[16] a) P. Gkoupidenis, N. Schaefer, B. Garlan, G. G. Malliaras, *Adv. Mater.* **2015**, *27*, 7176; b) J. T. Friedlein, M. J. Donahue, S. E. Shaheen, G. G. Malliaras, R. R. McLeod, *Adv. Mater.* **2016**, *28*, 8398; c) S. T. Keene, T. P. A. van der Pol, D. Zakhidov, C. H. L. Weijtens, R. A. J. Janssen, A. Salleo, Y. van de Burgt, *Adv. Mater.* **2020**, *32*, 2000270.
[17] a) S. Koneshan, J. C. Rasaiah, R. M. Lynden-Bell, S. H. Lee, *J. Phys. Chem. B* **1998**, *102*, 4193; b) P. Banerjee, B. Bagchi, *J. Chem. Phys.* **2019**, *150*, 190901.
[18] a) T. Plett, M. L. Thai, J. Cai, I. Vlassiouk, R. M. Penner, Z. S. Siwy, *Nanoscale* **2017**, *9*, 16232; b) Y. Saito, *Membranes* **2021**, *11*, 277; c) E. Quartarone, S. Davino, E. Lufrano, L. Coppola, C. Simari, I. Nicotera, *ChemElectroChem* **2023**, *10*, e202201148.